1 Introduction

Lipid bilayers are thin polar membranes composed of two monolayers of lipid molecules. These membranes are flat, flexible and usually tension-free sheets that form a continuous barrier around all biological cells. The cell membranes of almost all living organisms and many viruses are made of a lipid bilayer, as are the membranes surrounding the cell nucleus and other sub-cellular structures. The architecture or behavior of these membranes have been tested experimentally, as well as in different in silico experiments. In this report, we go further into the study of a classical bilayer membrane using the Dissipative Particle Dynamics (DPD) technique. The method itself and various aspects of the simulations are introduced in 2. Results concerning the behavior of the bilayer membrane under diverse conditions (tail length, tail angle, polarity) are then given in 3. Finally, a short discussion on the interesting aspects of the results, as well as on the limiting aspects of the method is given in 4.

2 Methods

2.1 Dissipative Particle Dynamics

All the simulations in this report were made using DPD. DPD is a stochastic simulation technique developped in 1992 by Hoogerbrugge et Koelman. In DPD, the particles (a.k.a 'beads') represent part of or whole molecules, or even fluid regions, rather than single atoms. It was primarily designed for rheology but has now been used in many different fields. It enables to simulate the moves of complex polymers in a solvent composed of way smaller particles. This type of system is indeed hard to simulate with classical methods since it couples phases having very different timescales. DPD allows for the modelling of these multi-scale systems by keeping only the information considered relevant to the simulated phenomenon. See [1] for more information about the technique and the last progresses made.

2.2 Why is DPD is appropriate for simulating a bilayer

Simulating a bilayer membrane is not a trivial task. Indeed, a cell membrane is usually made of millions of lipids interacting together, and it's therefore completely impossible to take into account the interactions of all the atoms composing these polymers, using for instance a molecular dynamic simulation. Moreover, we don't necessarily know the precise force fields in play on the system, and are generally interested in the global behavior of the system (i.e. not every chemical detail). On the other side, methods which are too coarse-grained aren't necessarily well suited either. Indeed, their level of detail is usually too low to catpure phenomena interesting at the mesoscopic level (e.g. a membrane would be simulated as a deformable 2D sheet with finite elements method, bringing no information about, for instance, its time fluctuations). DPD is therefore an intermediate method which allows to make the link between the microscopic and macroscopic scale. The use of beads instead of atoms enables the simulation of relatively large systems, and the fact that soft potentials are used instead of hard ones (e.g. Lennard-Jones potential) makes the system compatible with large integration steps, therefore to run simulations for long time scales.

2.3 Interactions and associated parameters

The choice of a DPD method has a few drawbacks, notably when it comes to defining the parameters ruling the interactions of the system we simulate. Indeed, the interaction between beads consist of three forces requiring two parameters for each pair of beads. These three forces are as follow.

First, there's the conservative force (giving an 'identity' to the beads) which is defined as (here for two beads of type i and j):

$$\mathbf{F}_{ij}^{C} = a_{ij}(1 - r_{ij}/r_0)\hat{\mathbf{r}_{ij}}$$

The parameter a_{ij} therefore sets the maximum repulsion between beads of type i and j. Note that it is only defined for a distance $r_{ij} < r_0$.

Second, there's the dissipative force (creating relative momentums between the beads), which is:

$$\mathbf{F}_{ij}^{D} = -\gamma_{ij}(1 - r_{ij}/r_0)^2(\hat{\mathbf{r}}_{ij} \cdot \mathbf{v}_{ij})\hat{\mathbf{r}}_{ij}$$

The parameter γ_{ij} can therefore be understood as the strength of dissipation between two beads. $\mathbf{v}_{ij}$ is the vector of relative speeds between the two beads.

Finally, there's the random force (destroying relative momentums betweend beads), written as:

$$\mathbf{F}_{ij}^{R} = \sqrt{2\gamma_{ij}k_BT}(1 - r_{ij}/r_0)\zeta_{ij}\hat{\mathbf{r}_{ij}}$$

Two supplementary constraints between beads are then added to handle polymers, each of them adding two parameters for each pair of beads. There's first the Hookean springs that tie beads together. The equation of their potential for bead i and $i+1$ is:

$$U_2(i, i+1) = 0.5k_2(|\mathbf{r}_{ii+1}| - l_0)^2$$

k_2 must therefore be interpreted as a spring constant, while l_0 should be understood as the unstretched length of the spring. Note that the parameters are here not subscripted with bead indexes (e.g. $k_{2_{ij}}$) since we choose to keep them identical for all pairs of beads.

The last potential to be defined is the chain stiffness acting between adjacent bead triples in a chain:

$$U_3(i-1, i, i+1) = k_3[1 - cos(\phi - \phi_0)]$$

k_3 must therefore be interpreted as a bending constant, while ϕ_0 is a preferred angle.

This means that for a system with three different beads like ours (water, hydrophobic tail and polar head), assuming we don't vary γ_{ij}, k_2 and k_3, nine different interaction parameters must be defined. In this work, we choose to parametrize the interactions of our system using the work of both Groot and Warren [2] and Grafmüller and al. [3], with sometimes *ad hoc* corrections. Note that the great majority of the parameters values were obtained by trial and error, showing the heuristic side of DPD. The values are as follow:

a_{ij}	**W**	**H**	**T**
W	25	35	75
H	35	25	50
T	75	50	25

The hookean spring parameters k_2 and l_0 are always set to resp. 128 and 0.5 while the chain bending stiffness k_3 is set to 15 and ϕ_0 to 0. γ_{ij} is kept at 4.5.

Note that some of these parameters (e.g. preferred angle, polarity of the last tail bead) will be changed further in the reports for experiments.

2.4 Simulation parameters

We simulate the system in a box of size $32^3 r_0^3$ where r_0 is the elementary unit of length (computed in next subsection). Since we choose a density of 3 beads per unit r_0^3, this makes a total of 98304 beads. We then simulate the systems for 200000 timepoints, with an integretion step of value $5 \cdot 10^{-3}$. Data is sampled every 100 timepoints and used to construct the values of the observable every 100000 timepoints. These values should be large enough because of the soft potentials used in DPD, causing the correlation times for bead properties to be usually very short (cf. [4]).

However, we need to be sure that the system is at equilibrium state after the first 100000 timepoints, at least in a classical case. We therefore simulate a bilayer made of $H_3(T_4)_2$ with a lipid beads density of 0.02, which we know should yield a perfect bilayer at equilibrium. We then plot the evolution of the (adimensional) pressure, temperature and diffusion coefficients of each bead with time. Results are given figure 1.

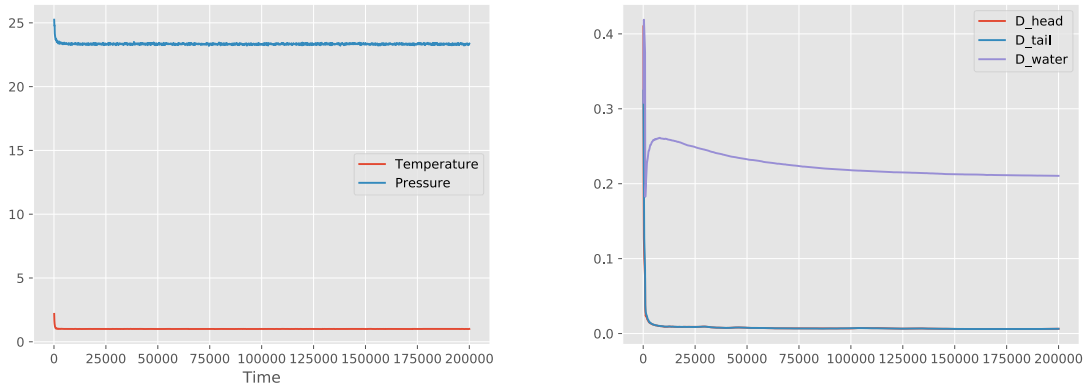

Figure 1: Evolution of the (adimensional) pressure and temperature (left) and diffusion coefficients of tail, head and water beads (right) for a lipid bilayer made of polymers with the architecture $H_3(T_4)_2$

Temperature and pression are cleary stabilized after just a few hundreds timepoints. Things take more time for the diffusion constants, but we can consider that the system is more or less at equilibrium after 200000 timepoints. However, since the simulations are very time-consuming, we make a large approximation and say that the system is at termodynamical

equilibrium after only 1000000 timepoints. We therefore ignore the first 1000000 timepoints in further results, in order to let the system relax to its (quasi) equilibrium state.

2.5 Computation of reduced units

Since DPD doesn't deal with real 'objects' but rather beads, the units we obtain must be rescaled to correspond to real quantities. If we manage to find the elementary unit of length (r_0) and of time (t_0), it's then possible to find all the other units, namely that we are studying a system at equilibrium in the canonical ensemble.

In order to find r_0, we follow the following procedure: we generate simulation with progressively increasing area per lipid (computed as the quotient of the membrane surface, i.e. product of the first two coordinates of the box size, and the number of lipids in the box). From this we get a result corresponding to an area per lipid in units of r_0^2. We then look at simulations corresponding to a null surface tension, meaning that the membrane is at equilibrium (as in biological conditions). Now, from experiments, we already know that a lipid area from a tension-free cell membrane should be around $0.65nm^2$ (of course, this depends on the lipid, but we keep this value as we're only interested in qualitative results). Therefore, the formula to obtain r_0 is simply:

$$r_0 = \sqrt{\frac{A_{exp}}{A/N}}$$

Where A is the simulated area of the box, N is the number of lipids simulated and A_{exp} is the experimental area of a lipid.

Similarly, we know that the dimensionless diffusion constant can be written as:

$$D' = \frac{Dt_0}{r_0^2}$$

Since we know from the literature that a typical lipid diffusion constant is about $1\mu m^2/s$ (see [5]), we can quite easily compute the value of t_0 if r_0 is already known.

3 Results

3.1 Initial model

Out of simplicity, we start by simulating a simple amphiphile architecture for which interesting results could be obtained in the past. In this architecture, the lipid polymer is composed of three polar heads and two hydrophobic tails, each of which being attached to a different head. We denote this architecture by $H_3(T_4)_2$.

The first experiment we lead is to look for the fraction of lipid beads (which, out of simplicity, we'll abusively call lipid beads density from now on) required to find a membrane with no surface tension (as observed in biological membranes). We therefore follow the procedure explained in 2.5 and launch a grid-search on a cluster which allows to explore the lipid beads density space.

Figure 2 gives the evolution of the adimensional surface tension, i.e. $\frac{\sigma r_0^2}{k_b T}$ with the fraction of beads lipids in the simulation (from which we can easily extract the corresponding number of lipids, the size of the box remaining constant of size $(32r_0)^3$).

Several observations can be made from this plot. First, we acknowledge that the surface tension gets close to zero for a lipid fraction of about 0.02, corresponding to an area per lipid of $1.255r_0^2$. This yields the value $0.72nm$ for r_0.

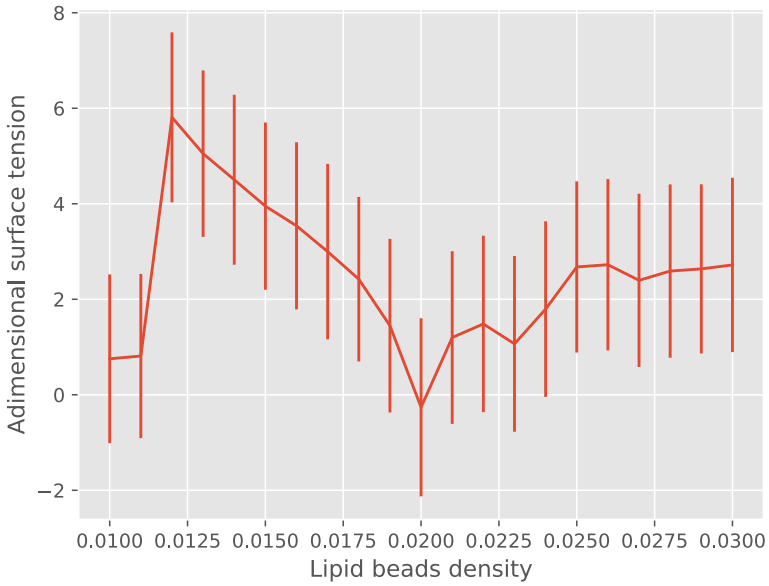

Figure 2: Evolution of the (adimensional) surface tension with the lipid bead density for the polymer architecture $H_3(T_4)_2$

What is interesting is that the evolution of the surface tension is not linear at all. In order to have a better understanding of the situation, we plot the membrane for a lipid beads density of 0.01, 0.02 and 0.03. Results are given figure 3. The strange evolution of the surface tension can thus be explained by the following phenomena: when the lipid density is too low, then pore(s) start(s) forming and the tension can remain reasonably low as the total volume occupied by the membrane is smaller than required. However, as the density increases, pores starts resealing, and a compromise must be found between the tail hydrophobicity and the still low number of lipids, eliciting a large area per lipid and therefore a large surface tension. The area per lipid then starts decreasing until a perfect bilayer is formed. Sill increasing the density firsts provoke a bending of the membrane, the area per lipid becoming low. If the density keep increasing, the a third layer start assembling so that the total free energy of the system remains reasonable.

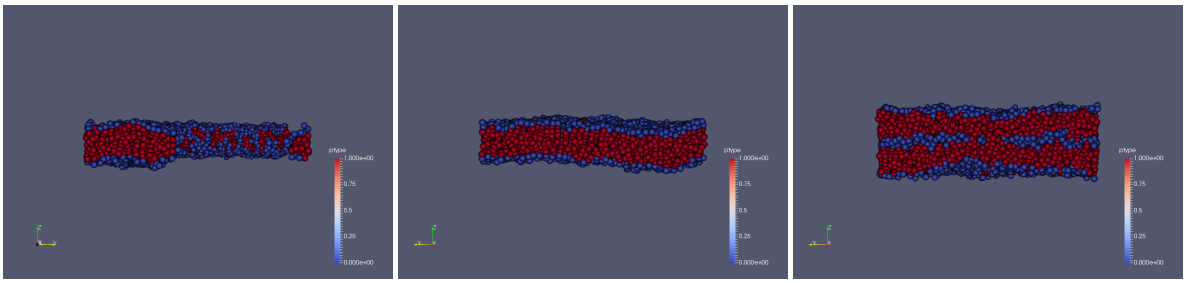

Figure 3: Representation of the membrane for the polymer architecture $H_3(T_4)_2$ for lipid bead density of 0.01 (left), 0.02 (middle) and 0.03 (right).

If we know get interested in the diffusion constant of the lipids for the tension free membrane, we find $D' = 6.4 \cdot 10^{-3}$, which yields the approximate value $3ns$ for t_0.

Finally, if we look at the density and stress profiles of the tension-free membrane, we get results very similar to what can be found in the literature. The results are given figure 4.

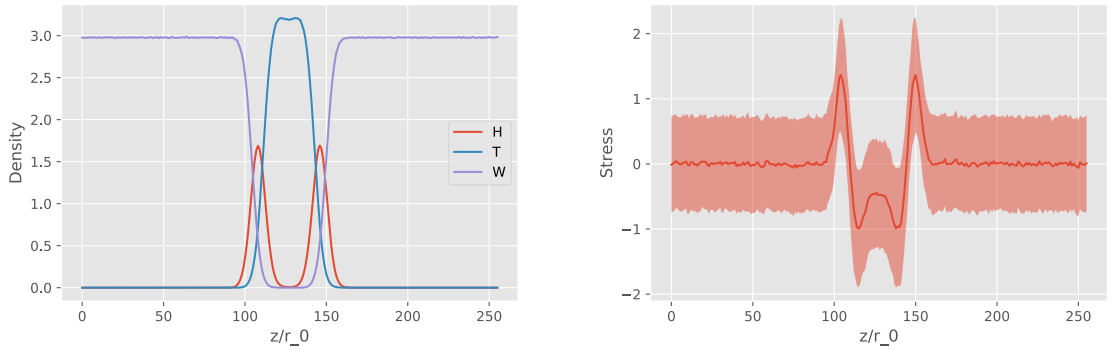

Figure 4: Representation of beads density profile (left) and the stress profile (right, std. in light red) for the tension-free bilayer made from the lipid polymer $H_3(T_4)_2$.

As expected, when progressing along the axis normal to the membrane plan, the density is first high in water beads (out of the bilayer), then the head bead density peaks (at the surface of the bilayer) while the water density drops, and finally the tail bead density increases a lot, even exceeding the one of water outside of the membrane. We also notice the small dip in the middle of the membrane, due to the fact that the lipids from both side of the membrane do not interdigitate. As for the stress profile, the results are also very conform to previous literature: the stress is more or less null in pure water areas, then increases a lot in the water-head area, and then get completely reversed in the head-tail area, to finally decrease again in the hydrophobic area composed uniquely of lipid tails. Note that there's a small difference with, for instance, what can be found in [4] as the central trough is missing. It's reasonable to hypothesize that this difference is due to the use of different lipid polymers.

3.2 Self-assembly of the bilayer

Self-assembly of lipids bilayer has already extensively been studied with DPD in the past (cf. e.g. [6]). It felt interesting to see if was possible to observe such a thing with our current set of parameters. Indeed, previous simulations in this report were made with beads disposed in an initial state such that the lipid bilayer was already formed. But what if we start from a completely random initial condition? Since the bilayer corresponds to the system state with the least free-energy, the membrane should spontaneously assemble if we simulate it for enough time. But things did not work as planned, as illustrated by figure 5.

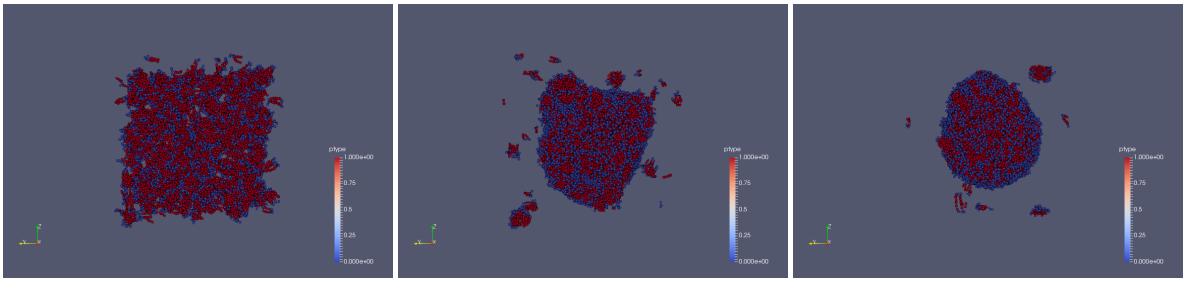

Figure 5: Spontaneous structure formation with the polymer architecture $H_3(T_4)_2$ at time $t = 1000$ (left), $t = 10000$ (middle) and $t = 200000$ (right)

Clearly, the system tends to form pseudo-spheroidal vesicles instead of a bilayer. This shape probably corresponds to a local equilibrium in which the simulation is stuck. Increasing the temperature, or manually perturbing the system could maybe improve the results. It is also very likely that a way longer simulation time is necessary to obtain a membrane. There are actually a lot of reasons which could explain why the simulation did not work, and some interesting points are raised in the reference [6], but this is not the object of this report.

3.3 Impact of the tail length

We now get interested in the impact of the length of the lipid tails. In order to see how the number of tails beads (which seems like a good proxy for tail length) impacts the results, we study polymers of the type $H_3(T_i)_2$ with i ranging from 0 to 19. These configurations lead to stable membranes for $i \geq 3$, with, as expected, an increasing hydrophobic volume in the membrane. Density profiles for $i = 1, i = 8$ and $i = 19$ are shown figure 6

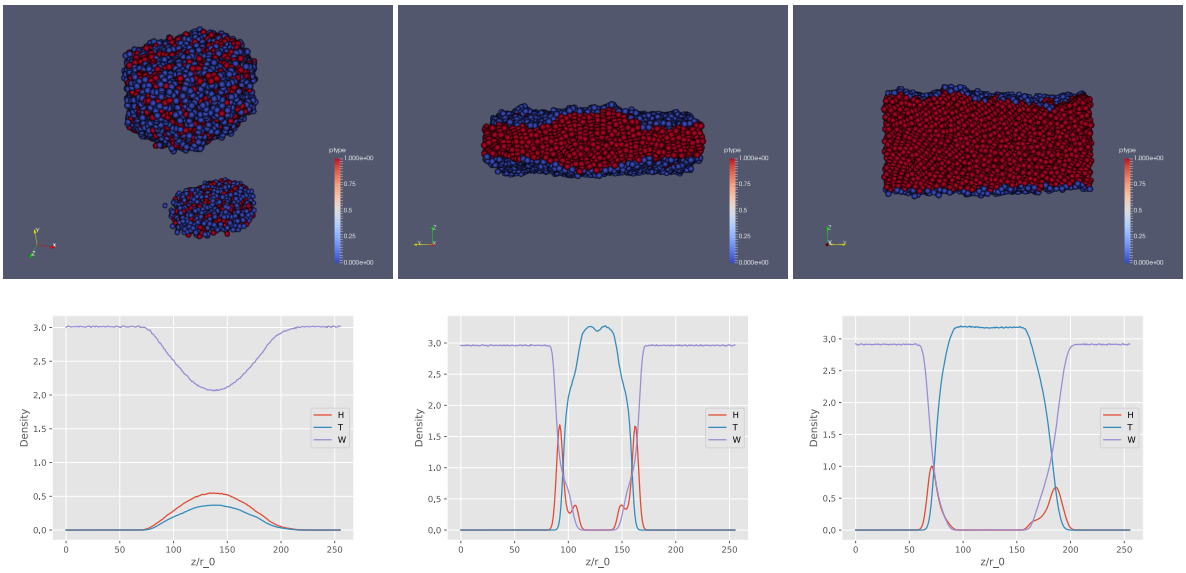

Figure 6: Representation of the membranes and associated beads density profile for the bilayer made from the lipid polymer $H_3(T_1)_2$ (left), $H_3(T_8)_2$ (middle), $H_3(T_{19})_2$ (right).

These profiles are very expectable, but two interesting phenomena can be noted. The first one is that the dip between the two tails end almost disappear for very long tails (as illustrated on figure 6, bottom right). The second one is that the membrane structure become less homogeneous with long tails. This can be observed on both figure 6, top middle, and on the density profile on bottom right.

Figure 7 (left) shows that the end-to-end length of the lipid polymers increases linearly with the number of beads. And as shown in the literature, the end-to-end length of the lipid polymers is more or less half the membrane size (note however that the results are biased toward a ratio of about 1.6 instead of 2, with no obvious reason why), as shown on figure 7 (middle). It is important to mention here that the surface tension is affected by the tail length, and since the lipid bead density was no adapted to keep it constant, the previous results were not obtained on tension-free membranes. As illustrated on figure 7 (right), the only result with a tension-free membrane was obtained for the previously used $H_3(T_4)_2$. It was however computationally too expensive to run the experiment varying both the bead density and the number of tail beads at the same time.

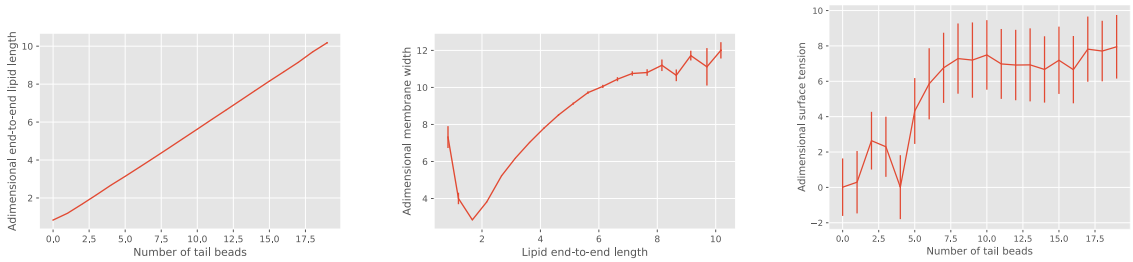

Figure 7: Left: Evolution of the lipid end-to-end length with the number of beads. Middle: Evolution of the membrane width against the end-to-end length of the lipids. Right: Evolution of the surface tension with the number of tail beads

3.4 Impact of the tail angle

To explore how the model behaves in less realistic conditions, it seemed interesting to see how the tail angle impacts the membrane. We therefore vary the angle HTT (i.e. between the head bead and the first and second tail beads) from 0° to 180°.

We first look at how the bead density profiles evolve. The results are shown figure 8.

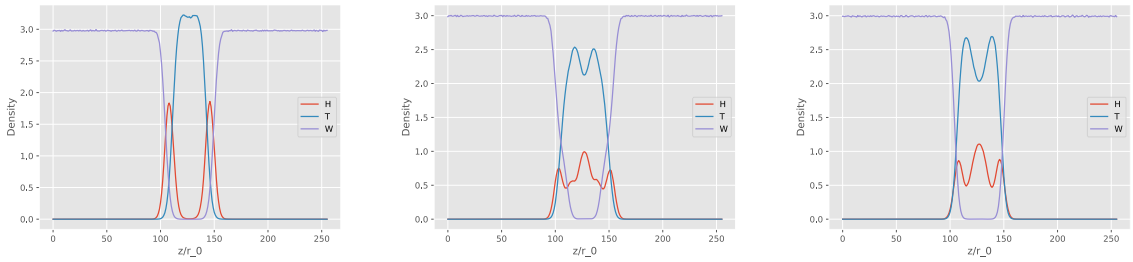

Figure 8: Representation of the beads density profile for the bilayer made from the lipid polymer $H_3(T_4)_2$ with a tail angle of 0° (left), 80° (middle) and 160° (right).

From the density profiles, it seems that even for large angles, the membrane remains stable, but that the central zone contains mixed heads and tails beads. A representation of the membrane with angle 160° is given figure 9 (left), confirming this hypothesis. We also note that the structural stress is way lower than before in the central area of the membrane (cf. 9 (right)) but more peaked in the zones corresponding to the outer layers.

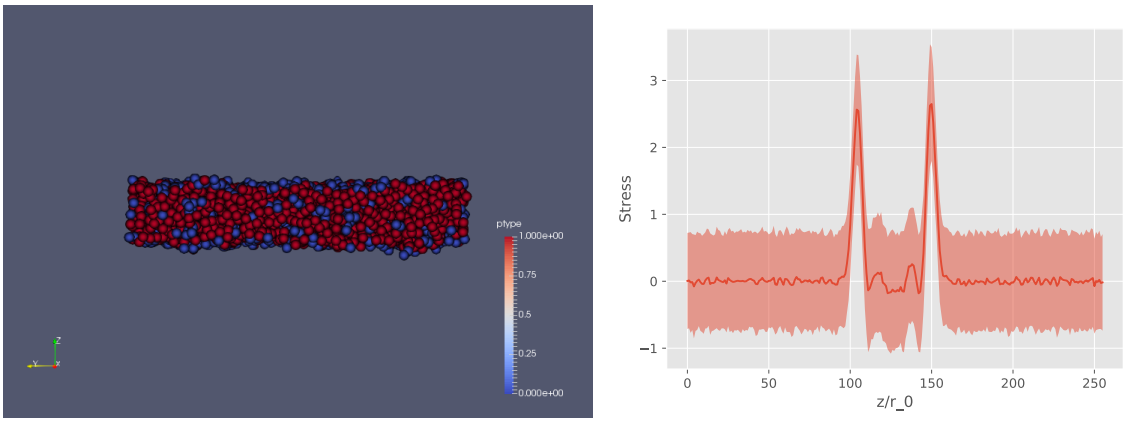

Figure 9: Representation of the membrane made from the lipid polymer $H_3(T_4)_2$ with a tail angle of 160° (left) and associated stress profile (right).

Finally, since the number of tail and head beads is the same, it is likely that the surface tension is not really dependent on the tail angle. Is that really the case? The evolution of the surface tension with the tail angle is given figure 10.

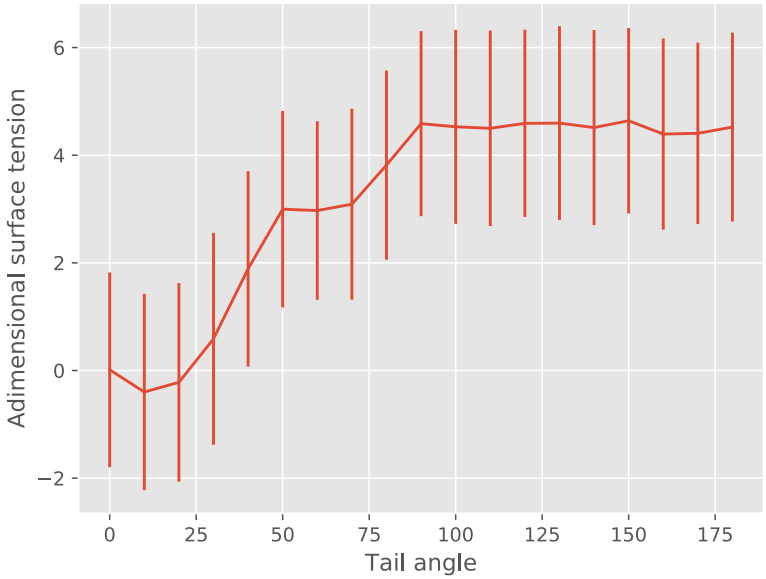

Figure 10: Evolution of the surface tension with the tail angle for the membrane made from the lipid polymer $H_3(T_4)_2$.

It therefore seems that the surface tension is indeed dependent on the tail angle, in a negative way for low angles (i.e. inferior to 20°) and in a positive way for large angles. However, we observe a phenomenon of saturation for very large angle (i.e. superior to 100°), for which the surface tension seems to stagnate even if the angle keeps increasing.

3.5 Impact of the polarity of the last tail bead

As a final experiment, we try changing the polarity of the last tail bead, from a water repulsion coefficient of 0 (i.e. extremely hydrophilic) to 80 (hydrophobic). For reference, the value used until now was 75. All the other interaction coefficients are kept similar to the ones of a normal tail bead.

Very interesting results are obtained. For pretty much all cases, a stable structure looking like a bilayer can be obtained. However, looking more closely at the results, it appears that the outer and inner layers of the membranes have been switched for interaction coefficients less than 30. This phenomenon seems actually quite logical since the last tail bead becomes more hydrophilic than the hydrophilic heads themselves, leading to a reversion of the lipids. Illustrations of the obtained membranes are given figure 11.

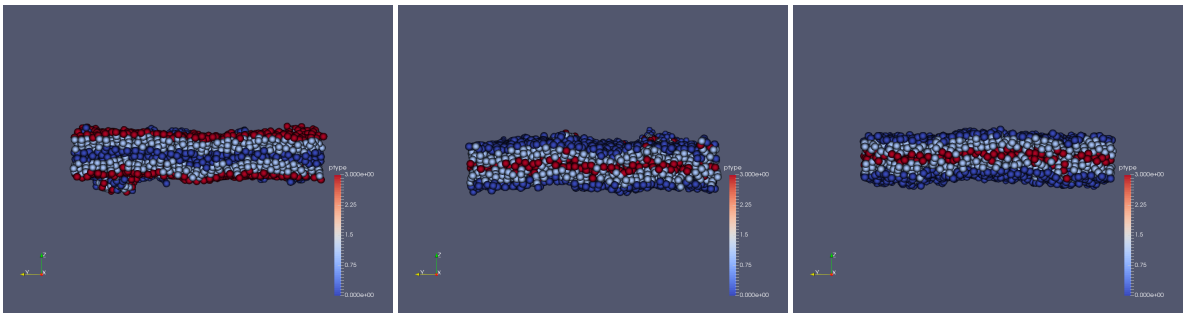

Figure 11: Representation of the membrane made from the lipid polymer $H_3(T_4)_2$ with the last tail bead having an increasing water interaction coefficient: 20 (left), 30 (middle) and 40 (right).

Figure 12 shows the progressive inversion of the membrane with time.

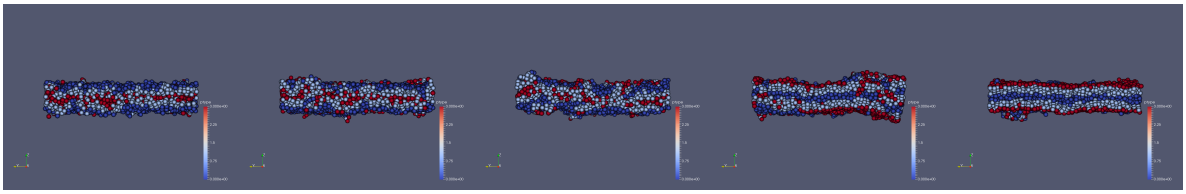

Figure 12: Progressive inversion of the membrane made from the lipid polymer $H_3(T_4)_2$ with the last tail bead having a water interaction coefficient of 20. Time shown (from left to right) are: 1000, 3000, 10000, 50000 and 100000.

Since for stable membrane, the structure is exactly the same as before, we expect the surface tension not to vary a lot with the polarity. Result is given figure 13, confirming this intuition. Note that the maximum surface tension is obtained when for the critical value 20, for which the membrane get reversed but very slowly.

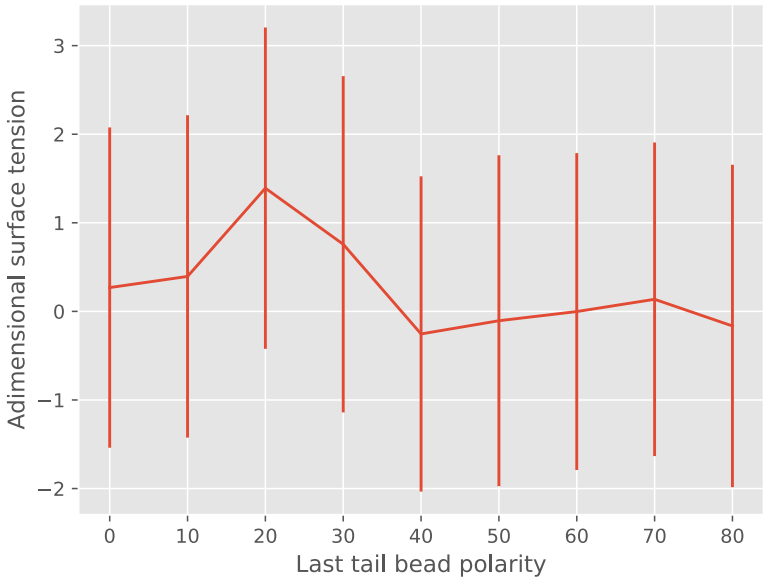

Figure 13: Evolution of the surface tension with the last tail bead polarity for the membrane made from the lipid polymer $H_3(T_4)_2$.

Finally, as a matter of illustration, it seemed interesting to plot the bead density profile of the reversed membrane. The following plot (figure 14) was obtained for an interaction coefficient of 10, 20 and 30:

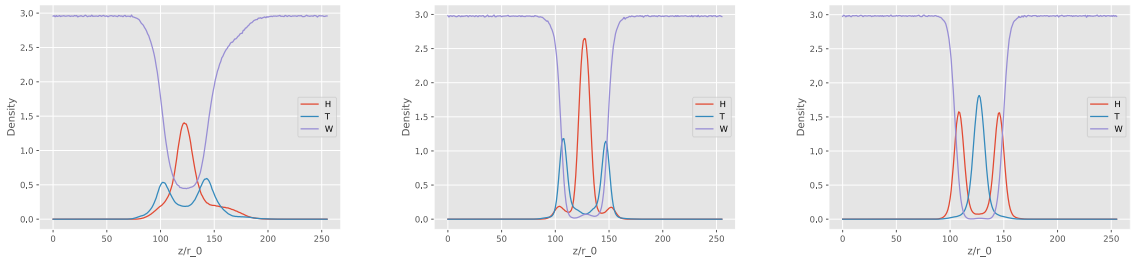

Figure 14: Representation of the beads density profile for the bilayer made from the lipid polymer $H_3(T_4)_2$ with an interaction coefficient of 10 (left), 20 (middle) and 30 (right).

It's interesting to acknowledge how, for very hydrophilic last tail bead, the water is progressively admitted inside the membrane.

4 Conclusion

Although DPD requires a little bit of tuning before being functional (heuristic derivation of the elementary units, obtaining of the interaction parameters by trial and error, etc.), it enables to simulate large systems quickly and for long time intervals, while keeping a good

spatial resolution. Indeed, it was not only possible to get back most results from the literature (e.g. beads density and stress profiles, evolution of the surface tension with the area per lipid, membrane width increasing linearly with the lipid end-to-end length, etc.), but also to explore a bit more in depth some parameters of the membrane. This enabled to discover that the membrane structure is quite resilient to even large head-tail angles, althought the hydrophobic area becomes filled with polar heads. Another interesting and not so intuitive phenomenon was the reversal of the membrane when changing the polarity of the last tail bead.

However, due to the fact that simulation were quite time-consuming, it was not possible to explore the system as in-depth as one could wish. Indeed, since grid-searches in two dimensions are already extremely greedy, it was not possible to tune both at the same time the lipid bead density and the tail length or tail angle. Yet this would have been extremely useful since this would have allowed to study tension-free systems, and therefore eliminate confounding factors due to the surface tension of the membrane. Similarly, we had to approximate the fact that the system was at equilibrium after 100000 timesteps, which was clearly not the case when looking at the evolution of the diffusion coefficient of the water beads. Finally, trying to fit our results to some experimental data could have been interesting, but wasn't possible because we did not possess such data. Leading the same experiments but with longer simulations, with tension-free membranes, and experimental data to compare our results to, would therefore be a very interesting extension of this work.

References

[1] Español, Pep and Warren, Patrick B., The Journal of Chemical Physics, 2017/05/24, 15, 150901, Perspective: Dissipative particle dynamics, 146, 2017

[2] Groot, R. D., & Warren, P. B. (1997). Dissipative particle dynamics: Bridging the gap between atomistic and mesoscopic simulation. The Journal of chemical physics, 107(11), 4423-4435.

[3] Grafmüller, A., Shillcock, J., & Lipowsky, R. (2009). The fusion of membranes and vesicles: pathway and energy barriers from dissipative particle dynamics. Biophysical Journal, 96(7), 2658-2675.

[4] Shillcock, J. C., & Lipowsky, R. (2002). Equilibrium structure and lateral stress distribution of amphiphilic bilayers from dissipative particle dynamics simulations. The Journal of chemical physics, 117(10), 5048-5061.

[5] Gaede, H. C., & Gawrisch, K. (2003). Lateral diffusion rates of lipid, water, and a hydrophobic drug in a multilamellar liposome. Biophysical journal, 85(3), 1734-1740.

[6] Marrink, S. J., Lindahl, E., Edholm, O., & Mark, A. E. (2001). Simulation of the spontaneous aggregation of phospholipids into bilayers. Journal of the American Chemical Society, 123(35), 8638-8639.